Melting point depression of Al clusters generated during the early stages of film growth: Nanocalorimetry measurements

S. L. Lai,[a] J. R. A. Carlsson, and L. H. Allen
Department of Materials Science and Engineering, University of Illinois at Urbana–Champaign, Urbana, Illinois 61801

This work investigates the thermodynamic properties of small structures of Al using an ultrasensitive thin-film differential scanning calorimeter. Al thin films were deposited onto a Si_3N_4 surface via thermal evaporation over a range of thicknesses from 6 to 50 Å. The Al films were discontinuous and formed nanometer-sized clusters. Calorimetry measurements demonstrated that the melting point of the clusters is lower than the value for bulk Al. We show that the melting point of the clusters is size dependent, decreasing by as much as 140 °C for 2 nm clusters. The results have relevance in several key areas for Al metallization in micro-electronics including the early stages of film growth and texture formation, the Al reflow process, and the dimensional stability of high aspect ratio Al lines. © *1998 American Institute of Physics.* [S0003-6951(98)04009-1]

The thermodynamic properties of material confined to small dimensions can be surprisingly different than the properties of bulk material due to the strong influence of the surface atoms. For example, the melting point T_m of nanometer-sized Au clusters is lower than the bulk value by over 500 °C.[1] Several recent articles[2–5] highlight the interest in the enhanced melting of small particles. Such properties of material are particularly relevant to the microelectronics industry, where the very large scale integrated (VLSI) technology requires device features to have tolerances of only a few nanometers by the year 2000.[6]

This letter investigates the thermodynamic properties of small structures of Al. The results have relevance in three key areas for Al metallization in microelectronics: (i) melting point depression as related to the Al reflow process,[7–10] (ii) coalescence during the initial stages of film growth as related to the formation of texture,[11] and (iii) dimensional stability of high aspect ratio Al lines in VLSI devices. For Al reflow, recent simulation studies have suggested that the lateral mass transport of Al at the surface is extremely high due to the premelting of the surface,[12,13] an idea related to the size-dependent melting phenomenon addressed in this letter.

Much has been learned about the size-dependent melting point depression in recent times. Studies in model systems like Au show that nanoscaled material simultaneously displays solidlike and liquidlike characteristics.[14] Other studies show that small systems can exhibit time-dependent structural instabilities,[15] even though the system as a whole is at thermodynamic equilibrium. As revealed by simulation studies,[14] the melting process initiates from the surface and is characterized by the increased mobility of the atoms in the top surface layers. The diffusion coefficient of these atoms approaches liquidlike values at temperatures much lower than T_0, the melting point for bulk material. Hasegawa *et al.*[16] computed the melting point of Al and found the melting point depression is similar to other metals (such as Pb). However, there has been little experimental evidence of melting point depression for Al.[17,18] In this work we use a calorimetric technique[19] to investigate the size dependence of T_m of self-assembled Al nanoclusters. To our knowledge this is the first experimental evidence for the melting point depression for Al clusters with a free surface.

The ideal technique for the measurement for thermodynamic properties is calorimetry.[19,20] This work is built upon our recent advances in calorimetry technique.[3,19,21] Our thin-film differential scanning calorimeter (TDSC) has extremely high sensitivity of 0.1 nJ, an ultrafast scanning rate of up to 10^6 °C/s, and a wide range in operating temperatures extending up to 700 °C. It is used *in situ* within a UHV system allowing for rigid control of sample preparation conditions. Described in its simplest form, the TDSC is a pair of thin metal strips, which function both as microheater and as thermistor when electrical current (I) is applied. By monitoring the change in voltage (V) of the strips, both the power $P = V \cdot I$ and the resistance $R = V/I$ of the strips are obtained. We obtain the temperature of the calorimeter using the temperature-resistance characteristics of the microheater, which are calibrated beforehand.[21] It is also calibrated internally by using the magnetic transition temperature of the Ni microheater itself as well as the melting point of thick (>200 Å) films, which have the bulk melting point $T_0 = 660$ °C for Al.

Calorimetry measurements of Al were made using the TDSC following the procedure described previously.[19] Al films were deposited onto a Si_3N_4 membrane via thermal evaporation, aligned to one of the two microheaters by using a shadow mask. The substrate was held at room temperature during Al deposition. The base pressure of the evaporation system was $\sim 1 \times 10^{-8}$ Torr and the deposition rate was 2–3 Å/s. Immediately after the deposition, *in situ* calorimetric measurements were performed. To begin the measurement, dc-current pulses were supplied to the two heaters simultaneously, thus raising the temperature of the microheaters at a rate of $\sim 1 \times 10^5$ °C/s by Joule heating. From the calorimetric measurements, the heat capacity C_p of the sample is readily obtained.

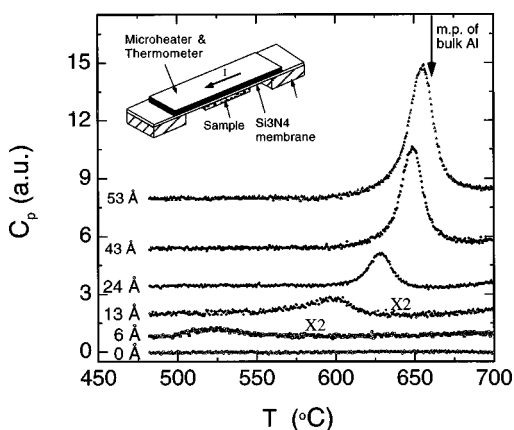---

[a]Electronic mail: s-lai@students.uiuc.edu

FIG. 1. The heat capacity C_p as a function of Al film thickness. The development of peaks is due to the melting of Al. Melting point T_m is determined using the position of ''melting peak.'' The inset shows schematically the TDSC used in this work.

Figure 1 shows the calorimetry results of a series of samples of thicknesses ranging from 0 to 53 Å as determined by the crystal monitor. The development of the peaks in the $C_p(T)$ curves is due to melting. We obtain the melting point T_m from the position of the ''melting peak'' in the $C_p(T)$ curve. Note that for smaller amounts of Al the value for T_m decreases. As expected, the T_m value approaches the bulk value as the amount of Al increases.

In order to relate the melting point with the microstructure of the film, we performed *ex situ* analysis of the films using a Phillips CM-12 transmission electron microscope (TEM). Planar TEM samples are prepared by positioning the membrane/sample assembly onto the standard copper TEM grid without sample thinning.

The TEM micrographs (Fig. 2) show that the Al film is discontinuous and forms a collection of individual nanometer-sized clusters. The process of nucleation and growth of three-dimensional Al clusters is characteristic of the early stages of film growth on the inert Si_3N_4 substrate. The Al forms self-assembled clusters in favor of a uniform layer as a consequence of the thermodynamic balance between the surface and interface energies.[22] Figures 2(a) and 2(b) show Al clusters on the Si_3N_4 substrate for samples with 6 and 20 Å of Al, respectively. By measuring the radii of individual clusters, histograms of a cluster size distribution are obtained as shown in Fig. 2(c). The cluster size exhibits an approximate Gaussian distribution, and hereafter we use the mean size of the distribution to represent the radius of the clusters for various amounts of Al deposited. The mean cluster radius for a film of 20 Å in thickness of Al is 67 Å.

The melting point T_m as a function of the size of the Al clusters is shown in Fig. 3. Note the reduction of the melting point as the particle size decreases. A decrease of 140 °C is observed for Al clusters with radii of ~ 20 Å. This is size-dependent melting point depression, as demonstrated in the Sn system by nanocalorimetry techniques.[3,19]

These results of size-dependent melting point depression are consistent with the two current models. The first model is based on classical thermodynamics and takes into account the surface/interface energies of a particle when evaluating the total free energy of the system. This model predicts that under equilibrium conditions each particle will consist of
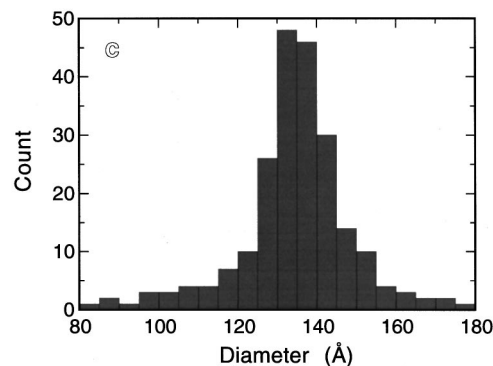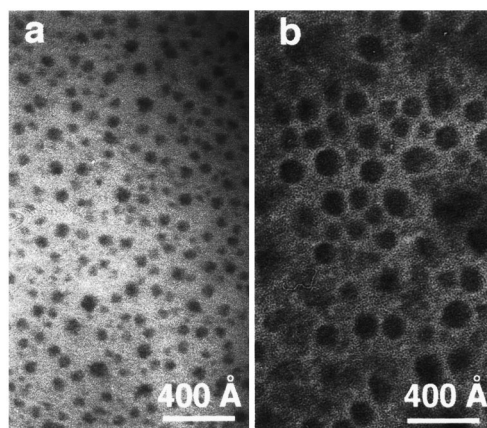

FIG. 2. TEM micrographs for ultrathin Al films of (a) 6 Å and (b) 20 Å in thickness. Nanometer-sized Al clusters are formed. (c) Histogram for cluster size distribution for a 20 Å thick Al films. An approximately Gaussian distribution is displayed, with the mean size located at $\bar{r} = 67$ Å.

two phases: a solid inner core and a liquid outer-shell layer.[23] The second model is based on the molecular dynamic methods[5] and evaluates the individual state of an ensemble of identical particles. In this approach, each particle fluctuates between the two states over long periods of time. At any one time, some of the particles will exhibit complete liquid-like structures while the remaining fraction of the particles exhibit complete solidlike characteristics. The time spent in each phase is related to the time-averaged fraction of material in each phase.

Following the classical thermodynamic model, the surface of a solid cluster begins to melt at temperatures below
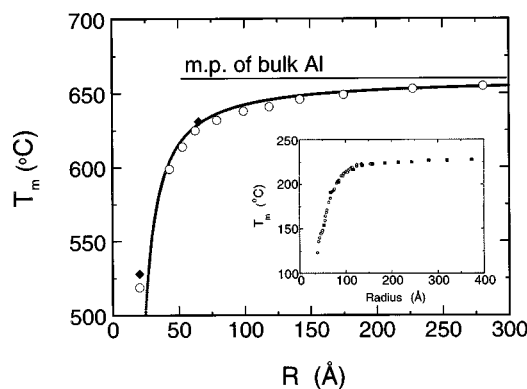

FIG. 3. The melting point as a function of Al cluster size. The solid line represents the best fitting to the experimental data using the liquid-shell model. The critical thickness of liquid-shell $t_0 = 12$ Å. The inset shows our previous results on Sn nanoclusters.

the bulk melting point forming a liquid shell surrounding the solid core.[3,23] Once the liquid layer thickness exceeds a critical value ''t_0'' the whole cluster melts homogeneously. The explicit expression of the melting point of a small cluster as a function of its size r can be written as[23]

$$T_0 - T_m = \frac{2T_0}{\Delta H_0}\left[\frac{\sigma_{sl}}{\rho_s(r-t_0)} + \left(\frac{\sigma_l}{r} + \frac{\Delta P}{2}\right)\left(\frac{1}{\rho_s} - \frac{1}{\rho_l}\right)\right], \quad (1)$$

where T_0 is the bulk melting point, ΔH_0 its latent heat of fusion, σ_{sl} and σ_l are the interfacial energies between solid and liquid and between liquid and its vapor, respectively, and ρ_s and ρ_s are the densities of solid and liquid, respectively. t_0 is the critical thickness of the liquid layer at T_m. ΔP is the difference between the vapor pressure at the surface of the liquid layer with an outer radius r at T_m and the vapor pressure at the flat liquid surface at T_0.

As predicted from the Eq. (1), there is substantial reduction in the melting point as the particle size decreases, which is consistent with our observations. By fitting our data to Eq. (1) and assuming the bulk values for $T_0 = 660\,°C$, $\rho_s = 2.55\text{ g/cm}^3$,[24] $\rho_s = 2.38\text{ g/cm}^3$,[25] and $\sigma_l = 914\text{ mN/m}$,[26] we obtain values for $\sigma_{sl} = 140\text{ mN/m}$ for the interface energy, which compares well with Turnbull's value $\sigma_{sl} = 93\text{ mN/m}$ obtained during the study of nucleation rates of the solid from liquid.[27] These values for σ_{sl} can be used to estimate the thickness of the liquid-shell layer. The range of values for $t_0 = 12–30$ Å, which we obtained, are much larger than the surface premelting thickness of $t_0 = 2$ Å measured for bulk Al.[28] However, this is expected since melting of small clusters is greatly enhanced due to the size effect.[3]

Melting point depression and the presence of disorder in small clusters will play a critical role in the evolution of microstructure during thin-film growth. In the early stages of deposition, each cluster grows incrementally (atom by atom) from a small cluster containing only a few atoms to a large cluster. Clusters must grow to a size of 10^6 atoms before exhibiting bulklike properties. During this growth process, each cluster passes through a wide range of values of properties, including changes in T_m, the amount of crystalline disorder, the latent heat of fusion, the surface energy, and the internal pressure. These changes will command a tremendous influence on the evolution of microstructure. For example, the development of crystallographic texture proceeds from the collection of small clusters containing little if any crystalline order to a continuous film which has preferred orientation.[11] This prompts the question—at what stage of growth does long-range order develop?

The size-dependent nature of the clusters also lends itself to possibilities of manipulating the path of growth of the film, since at any point in the deposition process there will be a distribution of cluster size, each size cluster having unique thermodynamic characteristics. Perhaps processing techniques (e.g., energetic ion beams and programed temperature cycles) can be used to stimulate (selectively) the growth of certain clusters based on size via the large difference in the thermodynamic properties of the clusters.

In summary, we have investigated the melting behavior of ultrathin Al films thermally evaporated onto a Si_3N_4 substrate. When the deposition thickness of Al is below 100 Å, the film is discontinuous and self-assembled nanometer-sized Al clusters are formed. We have found that the melting point of these small Al clusters is significantly reduced, by as much as 140 °C as compared to the bulk values. The experimental findings can be explained in the terms of current models. The results have relevance in several key areas for Al metallization in microelectronics.

[1] Ph. Buffat and J.-P. Borel, Phys. Rev. A **13**, 2287 (1976).

[2] G. Bertsch, Science **277**, 1619 (1997).

[3] S. L. Lai, J. Y. Guo, V. Petrova, G. Ramanath, and L. H. Allen, Phys. Rev. Lett. **77**, 99 (1996).

[4] M. Schmidt, R. Kusche, W. Kronmueller, B. von Issendorff, and H. Haberland, Phys. Rev. Lett. **79**, 99 (1997).

[5] B. Vekhter and R. S. Berry, J. Chem. Phys. **106**, 6456 (1997).

[6] K. N. Tu, J. W. Mayer, and L. C. Feldman, *Electronic Thin Film Science for Electrical Engineers and Materials Scientists* (Macmillan, New York, 1992).

[7] K. Kituta, Mater. Res. Bull. **11**, 53 (1995), and references therein.

[8] M. Inoue, K. Hashizume, and H. Tsuchikawa, J. Vac. Sci. Technol. A **6**, 1636 (1988).

[9] R. J. Baseman, J. Vac. Sci. Technol. B **8**, 84 (1990).

[10] C. S. Park, S. I. Lee, J. H. Park, J. H. Sohn, D. Chin, and J. G. Lee, IEEE VLSI *Multilevel Interconnecting Conference* 326 (1991).

[11] C. V. Thompson, Acta. Metall. **36**, 2929 (1988).

[12] K. Hirose, K. Kiuta, and T. Yoshida, Tech. Dig. Int. Electron Devices Meet. , 557 (1994).

[13] F. H. Baumann and G. H. Gilmar, Tech. Dig. Int. Electron Devices Meet. 557 (1994).

[14] F. Ercolessi, W. Andreoni, and E. Tossati, Phys. Rev. Lett. **66**, 911 (1991).

[15] P. M. Ajayan and L. D. Marks, Phys. Rev. Lett. **63**, 279 (1989).

[16] M. Hasegawa, K. Hoshino, and M. Watabe, J. Phys. F **10**, 619 (1980).

[17] F. O. Jones and K. O. Wood, Br. J. Appl. Phys. **15**, 185 (1964).

[18] N. T. Gladkich, R. Niedermayer, and K. Spiegel, Phys. Status Solidi **15**, 181 (1966).

[19] S. L. Lai, G. Ramanath, L. H. Allen, and P. Infante, Appl. Phys. Lett. **70**, 43 (1997).

[20] J. M. E. Harper, Ph.D. thesis, Stanford University (1975).

[21] S. L. Lai, G. Ramanath, L. H. Allen, P. Infante, and Z. Ma, Appl. Phys. Lett. **67**, 1229 (1995).

[22] M. Zinke-Allmang, L. C. Feldman, and M. H. Grabow, Surf. Sci. Rep. **16**, 377 (1992).

[23] K.-J. Hanszen, Z. Phys. **157**, 523 (1960).

[24] *Single Crystal Elastic Constants and Calculated Aggregate Properties: A Handbook*, 2nd ed. (The M.I.T. Press, Cambridge, 1971), p. 8.

[25] *CRC Handbook of Materials Science*, Vol. 1 (CRC, Cleveland, OH, 1981), p. 71.

[26] V. K. Kumikov and K. B. Khokonov, J. Appl. Phys. **54**, 1346 (1983).

[27] D. Turnbull, J. Appl. Phys. **21**, 1022 (1995).

[28] A. W. Denier van der Gon, R. J. Smith, J. M. Gay, D. J. O'Connor, and J. F. van der Veen, Surf. Sci. **227**, 143 (1990).